Research Article

Effect of different attributes of the mimic human lumbar spine biomechanics material structure change by finite element analysis

Da-Ping Qin[1,2] · Xiao-Gang Zhang[2] · Ming Son[1] · Hua Zhang[1] · Lin-Zhong Cao[1] · Wen-Tao Zhao[3] · Zhi-Peng Wang[2] · Shi-Wei Xu[2]

Received: 22 April 2021 / Accepted: 2 November 2021
Published online: 20 November 2021

Abstract
In this study, we compared stress changes and quantity effect relationships from 3D finite element models of normal and degenerative lumbar segments. We further defined the mechanisms causing alterations in mechanical stability the control of normal and degenerative lumbar segments using traditional Chinese medicine. The characteristics of the stress change and the quantity effect relationships of the three-dimensional finite element model of normal and degenerative lumbar segments were compared. The mechanism(s) leading to changes in mechanical stability and the intervention and balance between normal and degenerative lumbar segments of the traditional Chinese medicine was analyzed. The change trend of stress and strain was compared with the three dimensional finite element model under different motion states of normal lumbar vertebrae. A 3D-FEM of degenerative lumbar segments L4 ~ 5 of the human spine was established to simulate the physiological and pathological changes of the lumbar spine in response to flexion, extension, lateral bending and torsion. The stress changes in the normal and degenerative lumbar vertebrae were assessed through external force interventions and the response to TCM. Stress in the degenerative lumbar vertebrae changed according the external load. Stress and strain were compared in the FEM model under a range of motion states. Components of the human lumbar vertebrae including the cortical vertebrae, cancellous bone, endplates, fibrous rings, and facet articular processes were investigated. The elastic modulus of the nerve roots and the posterior marginal structures of the vertebral body increased with lumbar degeneration. Under stress trends in normal lumbar and different degrees of degenerative lumbar structures including cortical bone, loose bone, terminal plate, fiber ring, nucleus, small articular processes, nerve roots and posterior structures. In normal lumbar spine, 20%, 50%, 70% lumbar degeneration, 106 different lumbar anterior flexion 30 and posterior extension with different external forces showed that ANOVA F was between 3.623 and 11.381 and P changed between 0.001 and 0.05.It is clear that in the lumbar movement segments under different pressure intervention, the changes in the degree of degeneration are significantly different from each constituent structure, among which the trend of expected change between the constituent structures of the lumbar anterior flexion 30 is particularly obvious. The stress distribution in the intervertebral discs were influenced by TCM, and the space in the spinal canal enlarged so that nerve root stress decreased, vertebral body stress increased, and facet processes and pedicle stress in the posterior regions exceeded those of the anterior flexion position. The internal stress of the intervertebral disc increased in the flexion compared to the extension position, gradually increasing from top to bottom. The stress concentration point of the degenerative lumbar disc is significantly greater than the stress in the

Da-Ping Qin and Xiao-Gang Zhang contributed equally to this work.

✉ Da-Ping Qin, qindaping888666@163.com | [1]Gansu University of Chinese Medicine, No. 35, Dingxi East Rd Chengguan District, Lanzhou 730000, Gansu Province, China. [2]Affiliated Hospital of Gansu University of Chinese Medicine, No. 732, JiaYuguan West Rd Chengguan District, Lanzhou 730020, Gansu Province, China. [3]Yunnan University of Chinese Medicine, No. 1076, Yuhua Rd Chenggong District, KunMing 650500, Yunnan Province, China.

normal lumbar disc stress distribution area, and increases with the degree of degeneration. Compared with the load capacity of normal lumbar and mild (15% reduction), moderate (40% reduction) lumbar disc protrusion model in bending, extension, axial rotation, lateral bending, the results found that the load transmission of lumbar disc degeneration model to different degrees has also changed, so its compression stiffness, strain distribution and size are also different. TCM can improve and treat lumbar disc disease through its ability to regulate the mechanical environment of degenerative lumbar vertebrae. Compared to the FEM models of the lumbar vertebrae, lumbar degenerative changes could be assessed in response to alterations in the biomechanical environment. These findings provide a scientific basis for the popularization and application of TCM to prevent and treat spinal degenerative disease.

Keywords Biological materials · TCM · FEM · Lumbar motor segment · Biomechanics

Abbreviations

BMDLD	Biomechanical mechanism of degenerative lumbar degeneration
CT	Computed tomography
FEA	FEM
MIMICS	Medical image control system
DICOM	Digital imaging and communications in medicine
CAD	Computer aided design
ALL	Anterior longitudinal ligament
PLL	Posterior longitudinal ligament
ISL	Interspinous ligament
OF	Outmost fibrosus
SSL	Supraspinal ligament
LF	Ligamentum flavum
CL	Capsular ligament

1 Introduction

The effective prevention and treatment of degenerative spine disease and studies of the structural mechanics of the human spine are challenging. The spine and lumbar vertebrae bear heavy loads and mediate a wide range of physiological activities. Excessive or uneven loads in the lumbar vertebrae accelerate degeneration of the lumbar vertebrae, particularly in the L4 segment [1]

Lumbar degeneration is the major cause of lower back pain in adults globally. Up to ~ 5% of adults possess degenerative lower back pain and according to the range of anatomical structures of the spine, lumbar degeneration can be subdivided into intervertebral disc degeneration, endplate degeneration, articular process degeneration, vertebral body degeneration, and ligament and muscle degeneration, in which intervertebral disc, endplate, and facet joint degeneration strongly influence lumbar vertebrae biomechanics [2]. Models such as the 3D-FEM have emerged as important assessments of spine biomechanics. Since Belytschko and colleagues [3] first used FEM in 1974, FEM methods have been widely used in studies of lumbar vertebrae biomechanics. Anterior longitudinal ligaments, posterior longitudinal ligaments, and small articular capsule structures make the models both complex and realistic, permitting it to accurately reflect the mechanical action of spine motion and to reflect changes in load action mechanics in an array of injuries. Through the 3D-FEM, the thoracolumbar segment of the spine and its physiological and pathological features can be analyzed, including normal thoracolumbar segments, degenerative changes of the thoracolumbar vertebrae, and osteoporosis (OA). A systematic study of the mechanisms of dynamic mechanical changes in traumatic vertebral compression fractures was performed using this system [4–14]. The degenerative processes of lumbar spine motion segments are complex and lead to changes in overall mechanical models of the spine. To-date, the simulation of lumbar degenerative FEMs have focused on material characteristics and changes in the intervertebral discs. Predictions of the origin of disc degeneration and the identification of factors mediating disc destruction are of critical importance to future therapeutic interventions [15].

2 Material and methods

2.1 Subjects

Two normal male volunteers, aged 55 ± 10.2 years, with an average height of 170 ± 8.5 cm and an average weight of 70 ± 11.5 kg were selected. Volunteers provided informed consent to the trial and were approved by the Hospital Ethics Committee. The lumbar vertebrae were continuously scanned using a Siemens 128 slice spiral CT (Germany). Scanning conditions were as follows: 120 kV; 0.43 mm pixels; 0.625 mm slice thickness; and 351 layers. Images were stored directly using DICOM 3.0 standards.

2.2 Finite element model establishment and mesh generation

CT images were imported into Mimics10.3 and the appropriate azimuth and gray thresholds were selected. Saved files were imported into Geomagic Studio 9.0 reverse engineering software to further repair the model and include

the lumbar endplate, fibrous annulus and nucleus pulposus. The nucleus pulposus and the fibrous ring account for ~ 46% of the lumbar intervertebral disc. The thickness of the endplate was ~ 0.5 mm and the thickness of the cortical bone was ~ 1 mm [8].

HyperMesh 12.0 software was used to divide the mesh, and the volume model were generated by the point cloud phase, polygon phase and shape stage. Material attribute definition, boundary conditions and load definitions were used to pre-process the model. The model was built using post-processing software ANASYS11.0.

2.3 Stress distribution of the lumbar anterior flexion

The 3D-FEM model of the lumbar spine was used to simulate the physiological state of flexion. At the initiation of lumbar flexion, the stress mainly concentrates on the lower extremities of the upper lumbar spine and lower joint processes. With increases in flexion, the stress in the upper and lower lumbar vertebrae and the upper edge of the articular process increase whilst the end plate of the upper vertebral body strengthen. These changes mimic those of the actual lumbar flexion, fully highlighting the reliability of the model.

2.4 Material properties

According to related studies FEM verification [16–24], the mechanic parameters of each component of normal and intact L4 ~ 5 vertebral FEMs are shown in Table 1. The material properties of each structure were introduced into ANASYS 11.0.

2.5 FEM of the normal lumbar spine

Using the pretreatment function of ANASYS 11.0, the structure of the endplate, intervertebral disc, nucleus pulposus, anterior longitudinal ligament, posterior longitudinal ligament, ligamentum flavum, interspinous ligament and supraspinal ligament were established based on the spinal model. The model was meshed with appropriate element and material properties (Fig. 1). Following mesh division, the upper and lower facets were treated with contact units to ensure normal function and the maintenance of spinal structures. The establishment of the FEM and the degree of human spinal and lumbar motion segments were measured as previously described. Physical mechanics and material properties were used as a study reference.

Table 1 Unit types and material properties of each region of the lumbar spine

Group formation	Unit type	Modulus of elasticity /MPa	Poisson ratio	Sectional area / mm^2	Number of cells
Cortical bone	Solid185	12,000	0.3	–	9038
Cancellous bone	Solid l85	100	0.2	–	53,080
Posterior structure	Solid l85	3500	0.25	–	29,312
Cartilage endplate	Solid l85	25	0.25	–	2654
Nucleus pulposus	Solid l85	1.0	0.4999	–	4362
Fiber ring matrix	Solid l85	4.2	0.45	–	3600
Facet joint	Solid l85	3500	0.25	–	64
Arthrodial cartilage	Solid l85	25	0. 4	–	599
Fiber ring fiber	Link10	–	–	–	–
Outmost fibrosis	Link10	550	0.3	0.70	2400
Second floor	Link10	490	0.3	0.63	1200
Third floor	Link10	440	0.3	0.55	1200
Fourth floor	Link10	420	0.3	0.49	1200
Fifth floor	Link10	385	0.3	0.41	1200
Innermost structure	Link10	360	0.3	0.30	1200
Lacertus medius	Link10	7.8	0.3	24.00	10
Ligamenta longitudinale posterius	Link10	10	0.3	14.40	8
Ligamentum flavum	Link10	15	0.3	40.00	6
Ligamenta interspinalia	Link10	10	0.3	26.00	4
Ligamenta supraspinale	Link10	8	0.3	23.00	4
Ligamenta intertransversaria	Link10	10	0.3	3.60	6
Articular capsule ligament	Link10	7.5	0.3	30.00	8

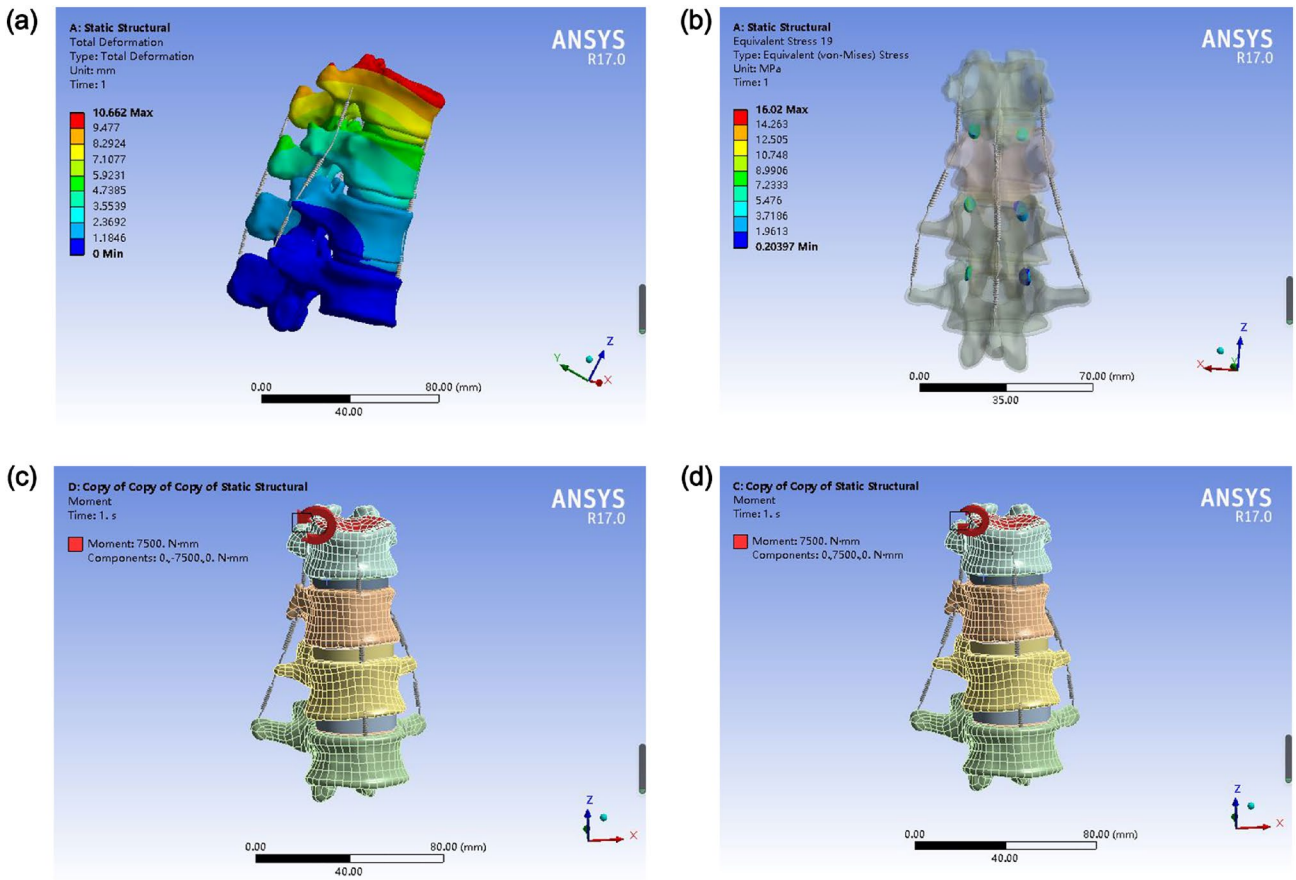

Fig. 1 Finite element model of the lumbar L4-5 vertebral body and intervertebral disc. **a** Left view; **b** posterior view; **c**-**d** anterior views

2.6 Mechanical methods

The 3D space position of the FEM was as follows: the *X*-axis faced perpendicular to the sagittal plane and the positive direction faced towards the left side; the *Y*-axis was perpendicular to the coronal plane and the positive direction was backwards; the *Z*-axis representing the longitudinal axis of the body and positive direction pointed to the head. The 3D-FEM of the lumbar motion segment was applied with a pulling pressing load. The positive direction of the *Z*-axis represented the direction of the drawing force; the negative direction of the *Y*-axis was directed according to pressure; and the positive direction of the *Z*-axis represented a horizontal stress state. The positive direction of the *Z*-axis deflected 30° in the negative direction of the *Y*-axis, representing a stress state of 30°. In the positive direction of the *Z*-axis, the *Y*-axis deflected 10°, and the stress state was extended 10° when the hand-pulling method was applied. The force increased from 400 to 700 N, and the force of pressing increased from 0 to 300 N. The linear law was 50 N. The design, implementation and evaluation of all experiments were performed by all authors. The main outcome measures were the stress distribution of the vertebral body and intervertebral disc, and the stress changes and displacement of the fibrous ring and nucleus pulposus.

2.7 Statistical analysis

Data were analyzed with SPSS 22.0 software. The analysis of variance or t-tests were used to compare data with normal distributions. Pairwise comparisons were used to measure LSD with $\overline{x} \pm s$, data enumerations of the χ^2 checkout, and ridit analysis of the grade data. The significant level was $\alpha = 0.05$. *P*-values ≤ were deemed statistically significant.

3 Results

3.1 FEM analysis of the degenerative lumbar vertebrae in response to different movements

Stress distribution analysis of the lumbar intervertebral discs in the different motion states showed that the disc formed the largest deformed structure during normal

spinal movement. The human disc is composed of the nucleus pulposus, the fibrous ring and the upper and lower cartilaginous endplates. The physical and chemical properties of the nucleus pulposus and fibrous ring changed according to disc degeneration, dehydration of the nucleus pulposus, relaxation and rupture of the fibrous ring. With increases in the degree of intervertebral disc degeneration, the elastic modulus of nucleus pulposus and fibrous ring symmetrically declined and eventually worsened. After rupturing the fibrous ring, the nucleus pulposus protruded and the compression of the nerve root promoted leg pain. Figure 2 shows the stress trends of the normal lumbar vertebrae and degenerative lumbar structures including cortical bone, cancellous bone, endplates, fibrous rings, nucleus pulposus, facet articular processes, nerve roots and posterior structures under different pressure. In the normal lumbar vertebrae, degenerative changes in the lumbar spine, a lumbar vertebrae anterior flexion of 30°, an extension of 10°of the lumbar vertebrae, and the effects of different external forces on the displacement of the components of the lumbar vertebrae were analyzed. The F values of ANOVA ranged from 3. 623 to 11. 381 g between 0.001 and 0.05. Clear lumbar motor segments under different pressure interventions were observed. These were obvious between the degree of degeneration and the displacement of each structure. The trend in change between 30° of the lumbar anterior flexion were most obvious. The stress concentration point of the degenerative lumbar intervertebral disc exceeded those of the normal lumbar intervertebral disc stress distribution area. The variation in degeneration increased. The FEM of normal and degenerative intervertebral discs has been reported by Yan and colleagues [25] found that the stress distribution of the degenerative intervertebral disc was larger, and that the circumferential fiber ring had greater stress. The stress of the nucleus pulposus also decreased. Fu and colleagues [26] reported similar data. The stress of the lower endplates of L3 and L4 of the intervertebral disc concentrated in central regions, whilst the stress of the degenerated disc focused on the posterior circumference of the endplate. We found that the stress of L3 and L4 superior articular facet of the degenerative intervertebral disc was significantly higher than that of the normal intervertebral disc. In addition, when the nucleus pulposus of intervertebral disc became degenerative, the intervertebral space became narrower, as did the anterior flexion of the spine. The bone cortex of the vertebral body degenerated, and the bone cortical hyperplasia near the intervertebral space increased in strength. The bone mass in the middle regions of the vertebral body decreased. The cortical depression of the anterior edge of the vertebral body was enlarged, and the load on the bone cortex of the anterior edge increased as the load transfer from the column moved forward [27]. Lissette and colleagues observed mild (disc height reduction: 15%) and moderate disc herniation (disc height reduction by 40%) during bending, stretching and axial rotation. The load transfer of the lumbar disc degeneration model also changed. This led to changes in the compression, stiffness, strain distribution and size of the region [26].

3.2 Analysis of axial displacement and joint motion of the L4-5 model under different motion states

A comparison of axial displacement clouds, forward flexion, extension, lateral bending and torsion of the L4Q5 model in different motion states is shown in Figs. 3 and 4. The variation of axial displacement in the L4Q5 model under different motion states was consistent with that reported in the literature [1] In addition, the forward flexion, extension, lateral bending and torsion angles of the model were similar to those previously obtained [28, 29] under 10 N m pure torque loading (Fig. 4). The finite element results of lateral bending assays were slightly smaller than the experimental data, but the overall trend of the range of lumbar vertebrae motion was consistent. Flexion is the key movement of the human spine with the largest range of motion. The torsion was limited due to the constraints of the facet joint [1].

In the *Y* axis, changes in the stress displacement curves of the lumbar intervertebral disc were most obvious. In the *Z* axis, the displacement of the lumbar intervertebral disc was maximal (Fig. 2). The distribution of stress in the vertebral and intervertebral discs initially appeared at the outer edge of the intervertebral disc and expanded in the direction of the flexion (Fig. 2). The stress displacement curves of the intervertebral disc from the outer edge to the central region were also assessed. The stress concentration point of the degenerative lumbar intervertebral disc exceeded those of the normal lumbar intervertebral disc. With increased degeneration, stress also increased. The stress-displacement curve of the lumbar intervertebral disc positively correlated with manual actions, but stress changes from the center of the intervertebral disc to the outer edge of the intervertebral disc increased. The stress-displacement curves of the nerve roots showed no positive correlation. An upward trend was observed during constant stress which decreased upon reaching the stress point. The center of the disc to the edges gradually enlarged and underwent torsional deformation. However, the stress-displacement curves of each component positively correlated under 10° extension loading (Fig. 2).

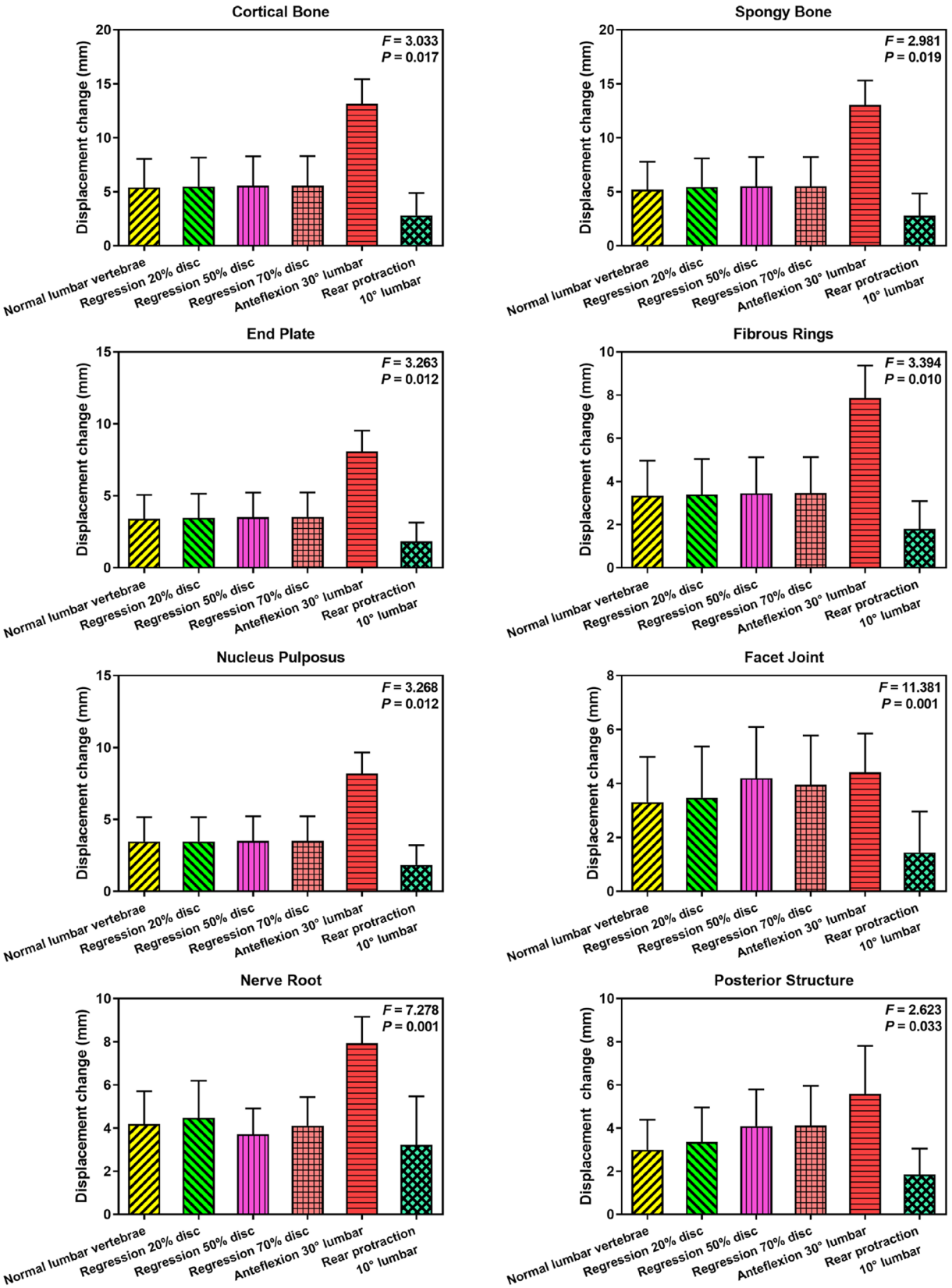

Fig. 2 Displacement of normal and degenerative lumbar spine structures under different load interventions

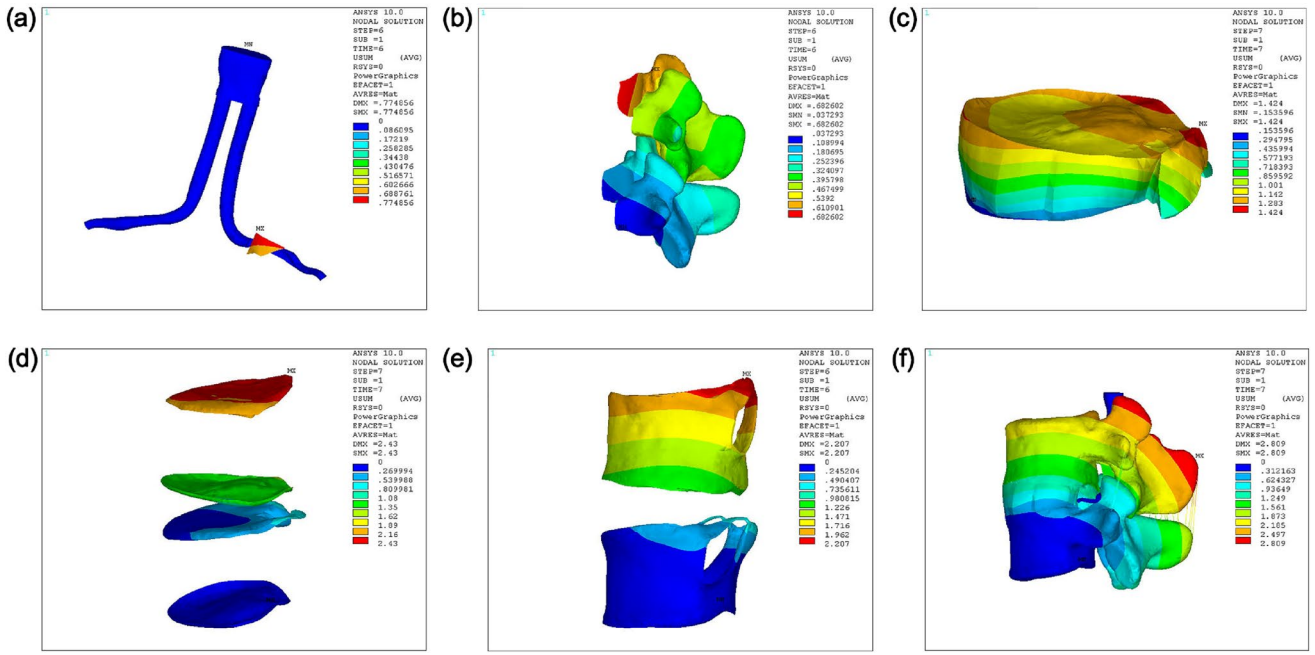

Fig. 3 Finite element model of the lumbar L4-5 vertebral body and intervertebral disc under different motion states. **a** The Finite element model of the nerve root; **b** Antexion; **c** Axial torsion; **d** extension; **e** The Finite element model of the intervertebral disc; **f** Methods used for the application of axial compression force

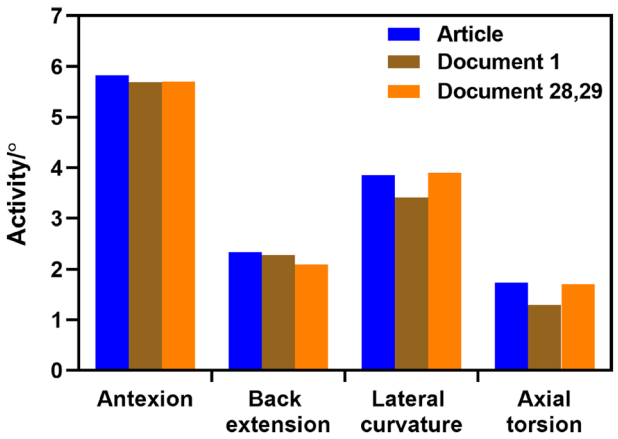

Fig. 4 Comparison of the range of motion for L4-5 vertebral bodies under different motion states

4 Discussion

TCM can effectively treat bone and tendon injuries. Here, to explore the mechanisms leading to lumbar degenerative disease, particularly lumbar disc herniation, and thus to improve spinal therapies, we performed 3D-FEM simulations [30], and assesses the stress-displacement trends of different lumbar vertebrae regions that had undergone degeneration. The stress status and clinical significance of the lumbar vertebrae during horizontal extension (10°), forward flexion (30°), lateral bending and rotation were also analyzed. Therapeutic mechanisms and safety ranges were also explored.

4.1 FEM for spinal massage studies

The basic principle of FEM is to divide the continuous elastic entity into numerous small elements. Due to the shape of small regional elements, the properties of the material can be determined. The properties of each small are studied individually and global properties of the elastic entity are obtained. The finer the division, the more accurate the calculations. FEM can thus be used to separate complex and irregular entities into different sizes and subtypes. FEM was first used to analyze structural mechanics in engineering and was introduced to clinical studies in the 1970s. It is now widely used in assessments of the lumbar vertebrae [31–34]. In recent years, combining computer technology and FEM with TCM techniques have advanced our knowledge of spinal massage manipulations [35–38]. By simulating spine stretching, bending and torsion, deformation, stress and strain can be assessed in response to a plethora of manipulations. Computer based mathematical models of Chinese massaging reproduce those of experimental conditions and provide quantitative and non-invasive evaluations of the functional state of lumbar vertebrae structures. This is advantageous over X-rays as the entire

waist can be imaged at a resolution comparable to CT scans of the lumbar appendage bone and soft tissue. This technique has broad applications for massage manipulations and avoids the potential side effects and cost of X-ray and CT procedures [36].

4.2 FEM of lumbar kinematics

4.2.1 Kinematic analysis of the lumbar vertebrae under different physiological loads

With the development of the finite element technique, kinematic studies on various physiological states of the lumbar vertebrae have been performed. Schmidt and colleagues [39] established the finite element model of the L4 ~ 5 segment to analyze changes in intervertebral disc stress, shear stress and fiber strain under complex loads. The results showed that the stress of the intervertebral disc was largest during flexion and smallest during lateral flexion. The maximum shear strain can be increased by lateral flexion or lateral buckling, and the maximum stress of the axial rotation fiber increased with extension. The maximum shear and fiber stress were concentrated on the rear side, and the stress increased according to the axial load, shear stress and fiber stress. Kozanek and colleagues [40] found that the neutral position of the facet joint rotates at an average of 2°or 6°and that the anteroposterior displacement was 2 mm during the flexion and extension of the lumbar vertebrae. The facet joint could not rotate and displace in the dominant direction under extension and rotation. A coupled motion of rotation and displacement (average ≤ 5° and 3 mm thick). Ayturk and coworkers [41] established the L4 ~ 5 spinal segment model and assessed the orthogonal mechanical properties of the fibrous ring in the physiological state. The results showed that loads of the fibrous ring were carried by collagen fibers under flexion, lateral bending and axial rotation. This was particularly evident in the areas of disc herniation. Kuo and colleagues [42] established of a finite element model of the lumbar vertebrae to analyze the biomechanical characteristics and stress of the lumbar facet joint and intervertebral disc. The results showed that under axial rotation, the stress of the facet joint was greatest at opposing sides. The stress of the lumbar intervertebral disc was significantly higher than that of the extension and axial rotation during flexion, but the stress of the facet joint did not change significantly. Qin and colleagues [43] constructed the L4 ~ 5 model. The stress concentration in the physiological segment of the lumbar vertebrae differed according to exercise conditions. The stress of the compact bone, pedicle, pedicle isthmus and posterior facet joint of the lumbar vertebrae were highest during axial compression (normal upper body load). The stress concentration of facet joint was higher in the lateral flexion vertebral body, intervertebral disc and posterior facet joint, but tension stress in contralateral side, posterior facet joint and posterior intervertebral disc were higher during rotation. The stress of the facet joint of the vertebral body and intervertebral disc were high during flexion and rotation. Kamińska and colleagues [44] constructed a lumbar vertebrae model of the lumbar spine load under different postures and upper limb loads. The results showed that the compression stress of the intervertebral disc increased with increasing loads, and that the increase of anterior flexion was more obvious that that of the vertical position.

4.3 Kinematics of the lumbar vertebrae following massage manipulation

TCM is an effective for the prevention and treatment of degenerative diseases of the human spine. In recent years, with the wide application of finite element techniques, have assessed massage combined with finite elements to establish models to study the biomechanical effects of massage on the lumbar vertebrae. This has revealed the timeliness and safety of the manipulations. To provide a theoretical and experimental basis for massage manipulation optimization, Xu and colleagues [45] analyzed the internal stress and displacement of the degenerative lumbar intervertebral disc. The results showed that the manipulations changed the displacement of the disc in the rotatory side, thereby relieving adhesion of the nerve roots, improving the symptoms of nerve stimulation. The safety and reliability of massage manipulations in TCM were then clarified. Wu and colleagues [46] compared the safety of straight lumbar rotational manipulations and lumbar fixed-point rotation techniques using the FEM model. The stress of intervertebral disc mainly concentrated on the outer fiber ring when using these manipulations. The stress distribution was focused in the facet joint and isthmus, the lateral recess of pedicle, the L4 spinous process and the upper articular process of the L4 upper edge and upper articular process on the left side of the L4 vertebra. The results revealed the practicability and scientific nature of Chinese massage manipulations. Hu et al. [47] massaged the lumbar pelvis and upper end of the femur under rotational manipulation of the lumbar vertebrae in the sitting position. The FEM model showed that the force of manipulations were related to changes in the anatomical structure of the corresponding areas of the lumbar vertebrae, and the manipulations could be performed under stable conditions. Yang and colleagues [48] used finite element methods to simulate changes in the internal structure of the lumbar vertebrae, and analyzed the mechanical effects of the manipulations in different positions. When the pressure increased to 300 N, the intervertebral disc

displacement amplitude peaked when the back extension reached 10°. These optimal therapeutic effects provide the basis for the clinical application of lumbar compression manipulations. Zhang and colleagues [49] found that, at a lumbar vertebrae flexion of 30°, displacements, strain and stress of the intervertebral disc tissue were obvious, suggesting that the 30° anterior flexion was safe and effective for the treatment of lumbar vertebrae disease. The position and selection of the lumbar vertebrae pull-extension requires further studies to determine the optimal position. Xu et al. [50] established the L4P5 finite element model to show changes of displacement and internal stress of the intervertebral disc acting on the lumbar oblique wrench method. The results showed that the stress of the intervertebral disc was smaller than that of the posterior structure of the intervertebral disc under manipulative action. The torsion vector from the center of the disc to the right side caused torsional deformation, and maximum displacement was located at the outer edge of the right side of the disc. Studies have shown that oblique wrenches in the intervertebral disc are safe, and that manipulations are more reasonable at the opposite side of the protrusion. At the same time, the disc protruded backwards during oblique compression, which was unsuitable for patients with lumbar spinal stenosis, which can guide clinical practice.

FEM is widely used in the analysis of problems related to the biological characteristics of the human spine. In TCM, massage manipulations of the lumbar spine and lumbar segment motion mechanics require analysis. On one hand, the mechanical and kinematic characteristics of the lumbar vertebrae under physiological conditions were assessed through the established, model. On the other hand, the stress trends of the lumbar vertebrae motion segments before and after manual interventions were revealed. Lumbar bone FEMs should now be expanded for more in-depth analysis of the treatment efficacy and treatment accuracy of TCM. Combined with the developmental models, rehabilitation medicine, such as acupuncture, guide function training and other mechanical effects on lumbar bone structure and disc function should be assessed. To-date, studies on soft tissue models of the lumbar vertebrae are sparse. More complete models can accurately reflect the relationship between normal mechanical actions in different stages of human spine movements and changes in the action mechanics of various injuries, to better explain the mechanism(s) of massage manipulation in TCM. Such analysis will provide a scientific basis to guide clinical practice [51, 52].

For the timeliness and safety of bone-regulating massages, the clinical efficacy of TCM in treating intervertebral disc herniation is clear, but for lumbar spinal stenosis and other patients with less buffer margins, particularly in patients with severe osteoporosis, manual therapy is inappropriate. The effects of oblique wrench on the lumbar vertebrae were studied through biomechanics and computer FEM. The changes of displacement and internal stress of the lumbar intervertebral disc during manipulative action were used to guide clinical treatment and reduce adverse reactions. Clinical studies on the prevention and treatment of orthopedic disease using TCM can also be performed. This provides a new platform and foundation for studies on the precision, targeting, visualization and digitization of TCM.

Acknowledgements We thank American Lin Editor who provided language editing services. We also thank the Gansu University of Chinese Medicine for supporting this study.

Author contributions DPQ and WTZ performed the literature search and selected patients. DPQ, WTZ, ZPW and SWX performed the experiments and extracted data. HZ, MS and LZC collected and collated clinical imaging data. DPQ and XGZ conceived the idea, designed the study, and critically revised the manuscript for intellectual content. DPQ completed the mechanical and statistical analysis. All authors reviewed the paper and approved the final manuscript.

Funding This study was supported by the National Natural Science Foundation of China (No. 81760873); Project of Innovation Fund of Gansu Province (No. 2020A-073).

Data availability All datasets and files are available on reasonable request.

Declarations

Conflict of interests The authors declare that they have no competing interests.

Ethics approval This study was granted an exemption from requiring ethical approval by the ethics committee of the Affiliated Hospital of Gansu University of Chinese Medicine. The authors obtained patient consent prior to patient enrollment.

References

1. Fang XG, Zhao GP, Wang CX, Bai LL, Yan WT, Ma T (2014) Construction and analysis of finite element model of L4–L5 lumbar motion segment from CT images. Chinese J Biomech Eng 33(4):487–492 (**(in Chinese)**)
2. Ferguson SJ, Steffen T (2003) Biomechanics of the aging spine. Eur Spine J 12:S97–S103. https://doi.org/10.1007/s00586-003-0621-0
3. Belytschko T, Kulak RF, Schultz AB, Galante JO (1974) Finite element stress analysis of an intervertebral disc. J Biomech 7(3):277–285. https://doi.org/10.1016/0021-9290(74)90019-0
4. Yoganandan N, Kumaresan S, Voo L, Pintar FA (1997) Finite element model of the human lower cervical spine: parametric analysis of the C4–C6 unit. J Biomech Eng 119(1):87–92. https://doi.org/10.1115/1.2796070
5. Goel VK, Kong W, Han JS, Weinstein JN, Gilbertson LG (1993) A combined finite element and optimization investigation of lumbar spine mechanics with and without muscles. Spine 18(11):1531–1541
6. Wu JSS, Chen JH (1996) Clarification of the mechanical behaviour of spinal motion segments through a three-dimensional poroelastic mixed finite element model. Med Eng Phys 18(3):215–224. https://doi.org/10.1016/1350-4533(95)00027-5
7. Gilbertson LG, Goel VK, Kong WZ, Clausen JD (1995) Finite element methods in spine biomechanics research. Crit Rev Biomed Eng 23(5–6):411–473. https://doi.org/10.1615/critrevbiomedeng.v23.i5-6.20
8. Feng Y (2010) Biomechanical study of the effect of different lumbar fusion cage on adjacent segments. Chinese J Biomed Eng 29(5):717–723 (**(in Chinese)**)
9. Rohlmann A, Bauer L, Zander T, Bergmann G, Wilke HJ (2006) Determination of trunk muscle forces for flexion and extension by using a validated finite element model of the lumbar spine and measured in vivo data. J Biomech 39(6):981–989. https://doi.org/10.1016/j.jbiomech.2005.02.019
10. Xu H, Zhang M, Li Y (2005) Real-time measure of displacement and intra-stress of normal lumbar disc during simulating rotatory ma-nipulation in sitting position. Chinese J Rehabil Med 20(8):563–565 (**(in Chinese)**)
11. Wan K, Li Y (2006) Application of finite element method in lumbar spine research. Chinese J Bone Joint Injury 21(2):158–160 (**(in Chinese)**)
12. Qin JS, Yu W, Peng XQ, Jiang YG (2013) Three-dimensional finite element modeling of whole lumbar spine and its biomechanical analysis. J Med Biomech 28(3):321–325 (**(in Chinese)**)
13. Qin D, Zhang X, Nie W (2017) FEM on simulation of change characteristics in human lumbar vertebrae under different motion status. J Med Biomech 32(4):355–362 (**(in Chinese)**)
14. Zhao WT, Qin DP, Zhang XG, Wang ZP, Tong Z (2018) Biomechanical effects of different vertebral heights after augmentation of osteoporotic vertebral compression fracture: a three-dimensional finite element analysis. J Orthop Surg Res 13(1):32. https://doi.org/10.1186/s13018-018-0733-1
15. Liu Y, Chen Q (2007) Recent advance in finite element research of disc degeneration and lumbar intervertebral fusion. J Int J Biomech Eng 30(1):14–17
16. Lu YM, Hutton WC, Gharpuray VM (1998) The effect of fluid loss on the viscoelastic behavior of the lumbar intervertebral disc in compression. J Biomech Eng 120(1):48–54. https://doi.org/10.1115/1.2834306
17. Chen H, Xu H, Zhang M (2005) Real-time monitoring of internal stress of lumbar vertebra by means of sitting position rotation. Chinese J Clin Anat 23(4):420–422 (**(in Chinese)**)
18. Wang JL, Parnianpour M, Shirazi-Adl A, Engin AE (2000) Viscoelastic finite-element analysis of a lumbar motion segment in combined compression and sagittal flexion. Effect of loading rate Spine 25(3):310–318
19. Zhang X, Qin D, Son M (2013) Effects of stress distribution of the degenerative intervertebral disc during lumbar pulling and pressing manipulation by FEM. China J TCM Pharm 28(10):3108–3114 (**(in Chinese)**)
20. Faizan A, Sairyo K, Goel VK, Biyani A, Ebraheim N (2007) Biomechanical rationale of ossification of the secondary ossification center on apophyseal bony ring fracture: a biomechanical study. Clin Biomech 22(10):1063–1067. https://doi.org/10.1016/j.clinbiomech.2007.04.012
21. Xiang P, Du C, Zhao MY, Tian S, Wang LZ, Fan YB (2014) Modal analysis of human lumbar spine using finite element method. J Med Biomech 29(2):154–160 (**(in Chinese)**)
22. Chen SH, Zhong ZC, Chen CS, Chen WJ, Hung C (2009) Biomechanical comparison between lumbar disc arthroplasty and fusion. Med Eng Phys 31(2):244–253. https://doi.org/10.1016/j.medengphy.2008.07.007
23. Polikeit A, Ferguson SJ, Nolte LP, Orr TE (2003) Factors influencing stresses in the lumbar spine after the insertion of intervertebral cages: finite element analysis. Eur Spine J 12(4):413–420. https://doi.org/10.1007/s00586-002-0505-8
24. Su J, Zhao WZ, Chen BZ, Li B, He SW, Fang X (2010) Establishing finite element contact model of human L1–L5 lumbar segments. J Med Biomech 25(3):200–205 (**(in Chinese)**)
25. Yan JZ, Wu ZH, Wang XS, Xing ZJ, Zhao Y, Zhang JG et al (2009) Finite element analysis on stress change of the lumbar disc degeneration. Zhongguo Yi Xue Ke Xue Yuan Xue Bao 31(4):464–467 (**(in Chinese)**)
26. Fu S, Huang J (2012) Lumbar spine FEM and its clinical significance. Chinese Med Equip J 33(10):76–78 (**(in Chinese)**)
27. Liu G, Yi B (2010) Thoracolumbar vertebra osteoporosis of stress distribution and clinical significance. Jilin Med J 30(19):3126–3127 (**(in Chinese)**)
28. Markolf KL, Morris JM (1974) The structural components of the intervertebral disc: a study of their contributions to the ability of the disc to withstand compressive forces. J Bone Joint Surg Am 56(4):675–687
29. Markolf KL (1972) Deformation of the thoracolumbar intervertebral joints in response to external loads: a biomechanical study using autopsy material. J Bone Joint Surg Am 54(3):511–533
30. Li J, Zhang X, Yang X (2007) The examples on the manipulation of "three steps and three postures and nine practices" that professor Song Gui jie treats the prolapse of lumbar intervertebral disc. J GanSu Univ TCM 24(6):1–3 (**(in Chinese)**)
31. Chen J, Cai G (2001) Computer-aided engineering analysis. China press of railway, Beijing (**(in Chinese)**)
32. Zhao W, Su J, Chen B (2009) Application of FEM in lumbar spine biomechanical study. J Clin Rehabil Tissue Eng Res 13(30):5928–5930 (**(in Chinese)**)
33. Bao C, Liu J (2009) Innovative design on finishing device of double grooved Grinding wheel based on TRIZ. J Mach Design 26(9):62–64 (**(in Chinese)**)
34. Li LT, Xue HJ (2009) Investigation on the relation between sitting posture comfort and time by stress distribution analysis of L4–L5 centrum. Sci Technol Eng 9(9):2424–2428 (**(in Chinese)**)
35. Bao C, Liu J (2009) Lumbar spine subjected stress characteristic for operators using chain saw in forest harvesting and finite element analysis. Sci Silvae Sinicae 45(3):96–100 (**(in Chinese)**)
36. Li Y, Zhong S (2003) A new idea of basic research of spine massage: computer simulation and visualization technology. Chinese J Rehabil Med 18(7):431–432 (**(in Chinese)**)

37. Xu H, Zhang M, Xu D (2008) FEM of lumbar intervertebral disc action by means of three anterior flexural rotations. Chinese J Convalescent Med 17(2):65–67 (**(in Chinese)**)
38. Wang GL, Zhang MC, Li YK, Xu HT, Qiu GC (2008) Comparison of lumbar rotation manipulation in three lumbar flexion levels. J Cervicodynia Lumbodynia 29(1):24–26 (**(in Chinese)**)
39. Schmidt H, Kettler A, Heuer F, Simon U, Claes L, Wilke HJ (2007) Intradiscal pressure, shear strain, and fiber strain in the intervertebral disc under combined loading. Spine 32(7):748–755. https://doi.org/10.1097/01.brs.0000259059.90430.c2
40. Kozanek M, Wang S, Passias PG, Xia Q, Li G, Bono CM et al (2009) Range of motion and orientation of the lumbar facet joints *in vivo*. Spine 34(19):E689–E696. https://doi.org/10.1097/BRS.0b013e3181ab4456
41. Ayturk UM, Garcia JJ, Puttlitz CM (2010) The micromechanical role of the annulus fibrosus components under physiological loading of the lumbar spine. J Biomech Eng 132(6):061007. https://doi.org/10.1115/1.4001032
42. Kuo CS, Hu HT, Lin RM, Huang KY, Lin PC, Zhong ZC et al (2010) Biomechanical analysis of the lumbar spine on facet joint force and intradiscal pressure - a finite element study. BMC Musculoskelet Disord 11:151. https://doi.org/10.1186/1471-2474-11-151
43. Qin M, Chai S, Huang L (2010) Three-dimensional finite element model analysis of lumbar motion segment under different working conditions. J GuangXi Med Univ 27(3):417–419 (**(in Chinese)**)
44. Kamińska J, Roman-Liu D, Zagrajek T, Borkowski P (2010) Differences in lumbar spine load due to posture and upper limb external load. Int J Occup Saf Ergon 16(4):421–430. https://doi.org/10.1080/10803548.2010.11076857
45. Xu HT, Xu DC, Li YG, Zhang MC, Li YK, Wang GL (2007) Analyses of intra-stress and displacement of degenerate lumbar disc during simulating rotatory manipulation by finite element. Chinese J Rehabil Med 22(9):769–771 (**(in Chinese)**)
46. Wu S, Zhang M, Li Y (2010) FEM of the stress and displacement of lumbar vertebrae of two sitting rotations. Guangdong Med J 31(8):992–994 (**(in Chinese)**)
47. Hu H, Xiong CY, Han GW (2012) Finite element analysis of lumbar pelvic and proximal femur model with simulate lumbar rotatory manipulation. Zhongguo Gu Shang 25(7):582–586 (**(in Chinese)**)
48. Yang X, Zhang X, Li J (2013) A three-dimensional finite element model for simulating strctching and pressing manipulations on lumbar vertebrae. Chinese J Trad Traum Orthop 21(7):4–6 (**(in Chinese)**)
49. Zhang XG, Dong JH, Yang XF, Li JB, Li YH (2010) Biomechanical analysis of simulating pulling, extension and compression on the three-dimensional finite element model of lumbar segments. J Clin Rehabil Tissue Eng Res 14(22):4000–4004. https://doi.org/10.3969/j.issn.1673-8225.2010.22.003
50. Xu H, Li S, Liu L (2011) FEM of the intervertebral disc during lumbar obligue-pulling manipulation. J Clin Rehabil Tissue Eng Res 15(13):2335–2338 (**(in Chinese)**)
51. Xu H, Li S, Liu L (2011) FEM of the intervertebral disc during lumbar obligue-pulling manipulation. J Clin Rehabil Tissue Eng Res 15(13):2335–2338 (**(in Chinese)**)
52. Wang Y, Zhang Q, Liu K (2013) Advances in the application of finite element method in lumbar kinematics analysis. Chinese J Rehabil Med 28(7):688–690 (**(in Chinese)**)